Fabrication and Postmodification of Nanoporous Liquid Crystalline Networks via Dynamic Covalent Chemistry

Mulder, Dirk J.; Scheres, Luc M. W.; Dong, Jingjin; Portale, Giuseppe; Broer, Dirk J.; Schenning, Albertus P. H. J.

Published in:
Chemistry of Materials

DOI:
10.1021/acs.chemmater.7b01334

Publication date:
2017

CHEMISTRY OF MATERIALS

Communication

pubs.acs.org/cm

Fabrication and Postmodification of Nanoporous Liquid Crystalline Networks via Dynamic Covalent Chemistry

Dirk J. Mulder,[†,‡] Luc M. W. Scheres,[†,§] Jingjin Dong,[∥] Giuseppe Portale,[∥] Dirk J. Broer,[†,⊥] and Albertus P. H. J. Schenning*[,†,⊥]

[†]Department of Functional Organic Materials and Devices, Chemical Engineering and Chemistry, Eindhoven University of Technology, Den Dolech 2, 5612 AZ Eindhoven, The Netherlands

[‡]Dutch Polymer Institute (DPI), PO Box 902, 5600 AZ Eindhoven, The Netherlands

[∥]Zernike Institute for Advanced Materials, Faculty of Science and Engineering, University of Groningen, Nijenborgh 4, 9747 AG Groningen, The Netherlands

[⊥]Institute for Complex Molecular Systems (ICMS), Eindhoven University of Technology, P.O. Box 513, 5600 MB Eindhoven, The Netherlands

Supporting Information

Well-defined nanoporous polymers that exhibit a high porosity, low density, high specific surface area, and permeability are of great current interest due to their applications in areas as filtration, adsorption, ion conductivity, and drug-release.[1−4] The small pore size in these materials makes discrimination between molecules and ions based on size and shape possible. To tune the performance of these materials, efforts are made to control pore size, pore morphology, and pore chemistry.[5,6] Straight and well-defined pores are often desired for fast diffusion and size selectivity whereas tunable pore chemistry offers additional tools for enhancing selectivity.

In the past decade, self-assembled liquid crystalline systems have proven to be useful to prepare porous materials with pore sizes around 1 nm.[7,8] Both lyotropic and thermotropic liquid crystal polymers have been employed by incorporating polymerizable groups to the liquid crystalline moieties using columnar, lamellar, or bicontinuous cubic phases.[9,10] In lyotropic liquid crystals, pores are created and size controlled by ions and the solvent, i.e., water.[11,12] In thermotropic liquid crystals, nanopores have been created by so-called porogen templates that are hydrogen bonded to the polymer network and washed away to create the pores structured.[13−16] So far, most of the pores that have been made are based on negatively charged carboxylates[6,14,17] but there are some examples of neutral[13] or positively charged[18] pores. These prefunctionalization approaches limit the control over the size and chemical nature of the pores and the set of molecules and ions that can be separated.[6,17] Therefore, the control of pore size and the chemical tunability of the porous material remains a challenge.

Herein we report on a facile method to fabricate and postmodify nanoporous liquid crystal polymer materials by using dynamic covalent chemistry. Dynamic covalent bonds can form, break, and exchange under an external stimulus, like the addition of a catalyst,[19] change of environment (solvent),[20,21] or heat. For this reason, they are appealing to produce, e.g., adaptive and self-healing materials.[21,22] However, so far, the use of dynamic covalent chemistry in the fabrication and functionality of nanoporous materials is limited.[23] We describe the photopolymerization of a reactive thermotropic smectic LC monomer containing a bisimine porogen (Figure 1a, compound **1**) and a reactive cross-linker (Figure 1a, compound **2**) to yield a polymer film that after acid treatment contains reactive pore surface aldehyde functionalities.[17] By postmodification of these moieties with a variety of amines, the size and chemical nature of the pores can be tuned in a facile fashion (Figure 1e).

The newly developed reactive bisimine **1** was prepared in a two-step synthesis route starting from 4-(6-hydroxyhexyloxy)-benzaldehyde. First, a methacrylate ester was prepared, whereafter **1** was obtained from the condensation reaction of the aldehyde with 4-(2-aminethyl)aniline. A methacrylate was used instead of acrylate to prevent side reactions while synthesizing the bisimine. The bisimine based on 4-(2-aminethyl)aniline (compound **1**) exhibits a smectic phase in a suitable working temperature range (<120 °C, Figures S2, S3). Fully aromatic diamines were also investigated, but this resulted in bisimines with a higher mesophase temperature, increasing the risk of premature polymerization during further processing. Cross-linker **2**, which has a similar molecular length as bisimine **1**, was prepared analog to the procedure described in the literature.[24,25] By the formation of the diazonium salt of 1,2-bis(4-aminophenyl)ethane, and the subsequent hydrolysis of it, 1,2-bis(4-hydroxyphenyl)ethane was obtained. Subsequently, by Steglich esterification of the obtained diol with 4-(6-acryloyloxyhexyloxy)benzoic acid **2** was obtained. The full chemical and thermal characterization of **1** and **2** can be found in the Supporting Information.

To prepare the smectic liquid crystalline network, a mixture containing the bisimine (**1**) and diacrylic cross-linker (**2**) was used. Some cross-linking is needed to avoid disintegration of the layers when their central units are removed. It was found that 20 wt % cross-linker was sufficient to keep the layered structure intact after removal of the bisimine template after polymerization (vide infra). The addition of compound **2** led to a slight change in phase behavior of bisimine **1** (Figures S4, S5). Upon cooling from the isotropic phase, a nematic mesophase is observed from 120 to 117 °C. The mixture shows a smectic A

Received: April 3, 2017
Revised: July 12, 2017
Published: July 13, 2017

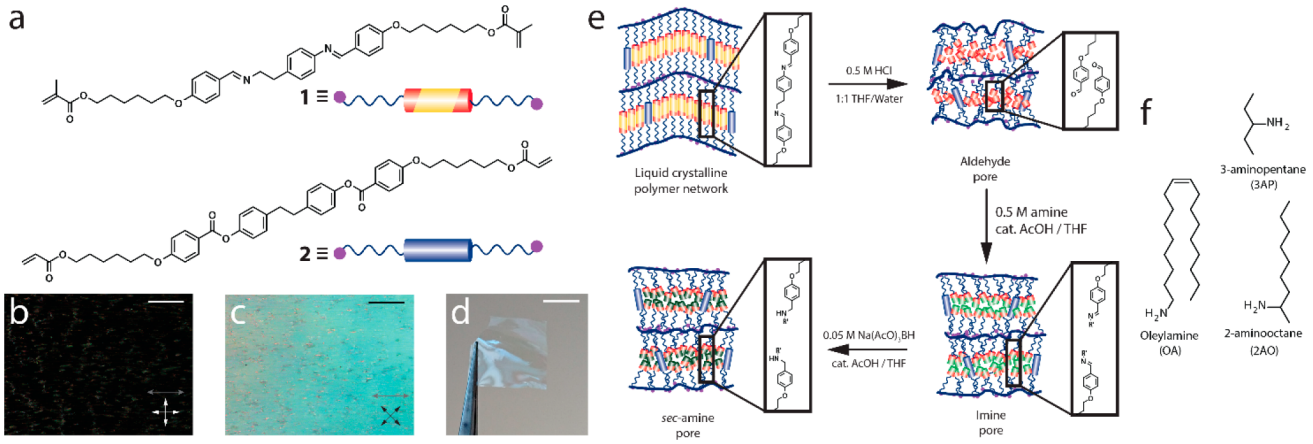

Figure 1. (a) Structures of the bisimine monomer (1) and the cross-linker (2). (b and c) Obtained smectic liquid crystalline polymer network between crossed polarized under 0° and 45° respectively. Scale bar = 250 μm. (d) Photograph of the smectic LC polymer film. Scale bar = 5 mm. (e) Schematic overview of the postsynthetic modifications of the LC network. (f) Amines that have been incorporated in the pore interior: 3-aminopentane (3AP), 2-aminooctane (2AO), and oleylamine (OA).

mesophase from 117 to 104 °C whereas a smectic C mesophase is present below 104 °C until 78 °C. Below this temperature, another tilted smectic phase was observed until −32 °C when crystallization sets in. To perform the photopolymerization, 1 wt % photoinitiator (Irgacure 819) and 0.5 wt % inhibitor (4-methylphenol) were added to the monomer mixture. The addition of inhibitor was necessary to circumvent premature thermal polymerization at elevated temperatures.

The photopolymerization was carried out in a homemade LC-cell provided with antiparallel alignment layer to obtain planar alignment. This is essential in order to obtain the pores orthogonal to the surface of the film after the later removal of the template. After the photopolymerization at 80 °C in the smectic C phase, the LC-cell was opened and the polymeric film was characterized. Transmission infrared spectroscopy confirms the conversion of the (meth)acrylatic C═C bonds of the monomers (Figure S1). Polarized light microscopy (Figure 1b,c) shows that the obtained polymer film is highly birefringent, which indicates a good alignment of the mesogenic moieties. X-ray diffractometry of the polymer film reveals a smectic organization of the molecules in the polymer network (Figure 2b). In the small-angle region of this plot, four small lobes can be observed corresponding to a typical smectic C chevron pattern. The spacing of the lamellae is 37 Å with a tilt angle of approximately 30°. Corrected for this tilt angle, a length of 43 Å is obtained, which is in agreement with the molecular length of compound **1** (43,3 Å, obtained by Chem3d minimization in stretched conformation).

To obtain a porous material with an aldehyde pore surface, the removal of the 4-(2-aminoethyl)aniline template was achieved by exposure of the network to a 0.5 M HCl solution in a 1:1 water/THF mixture overnight. The imine bonds were hydrolyzed and the diamine template was liberated from the polymer network. This was confirmed by transmission FTIR revealing a quantitative conversion of the imine groups to aldehyde functionalities (Figure 2a). No hydrolysis of the acrylate backbone was observed. The bisimine materials showed two distinct absorption bands at 1645 and 1625 cm^{-1} corresponding to the aliphatic and aromatic C═N stretch vibrations, respectively. The two peaks fully disappeared after the hydrolysis and a strong peak appeared at 1690 cm^{-1}. This vibration band is assigned to the C═O stretch vibration of the

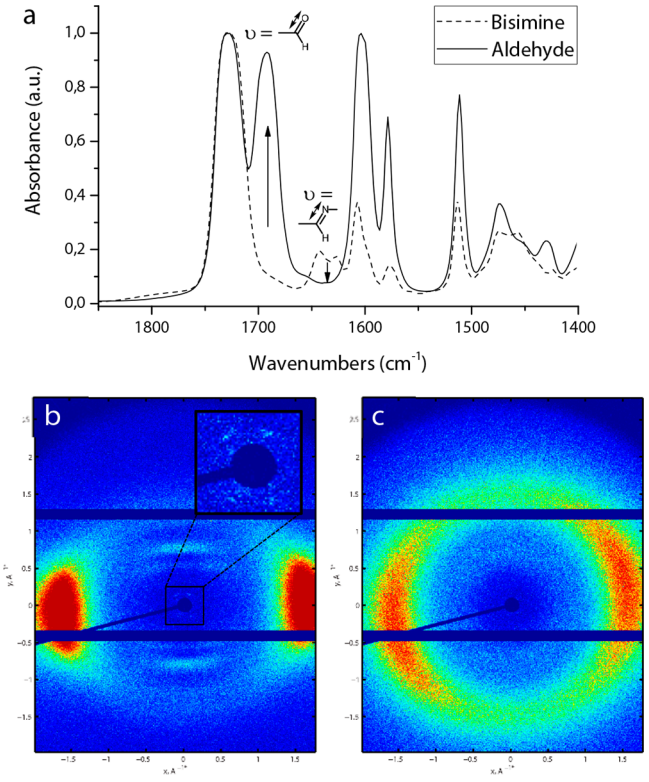

Figure 2. a) Transmission FTIR spectra of the bisimine (dashed) polymer and the aldehyde (solid) polymer network obtained after hydrolysis of the imine bonds. b and c) 2D X-ray diffraction patterns of the bisimine network and the aldehyde functional network, respectively.

aldehyde moiety, indicating an effective removal of the template and the formation of an aldehyde functional pore surface. X-ray diffraction of the dried films revealed that the lamellar ordered structure significantly reduced after removal of the bisimine template, whereas only the orientation of the molecules was maintained to some degree (Figure 2c and Figure S2 of the SI). Macroscopically, 29 ± 1% shrinkage, and 8 ± 2% swelling is observed along and perpendicular to the molecular director respectively, indicating the collapse of the lamellar structure and loss of the order of the initially aligned molecules.

DOI: 10.1021/acs.chemmater.7b01334
Chem. Mater. 2017, 29, 6601−6605

Despite the decrease in order, the obtained aldehyde functional polymer network was exposed to various amines to obtain new imine functionalities. To facilitate the reaction, a catalytic amount of acetic acid was added to the reaction mixture. Three different diamines, i.e., 3-aminopentane (3AP), 2-aminooctane (2AO), and oleylamine (OA), were used to obtain pores with different polarity and size. Interestingly, in each case, quantitative functionalization of the aldehyde pores was observed.

The FTIR spectra the complete disappearance of the C═O stretch vibration of the aldehyde moieties and a signal of the newly formed imine appears at 1645 cm^{-1} (Figure 3a). This result is explained by the fact that the network is reasonably flexible, which makes it possible to adapt to the guest molecules. Furthermore, the reaction was carried out in THF, wherein the network swells and forms pores. Most remarkably, the lamellar structure was recovered after the imine interior was obtained, and even more interesting, the layered nanostructure adapts to the size of the amine provided.

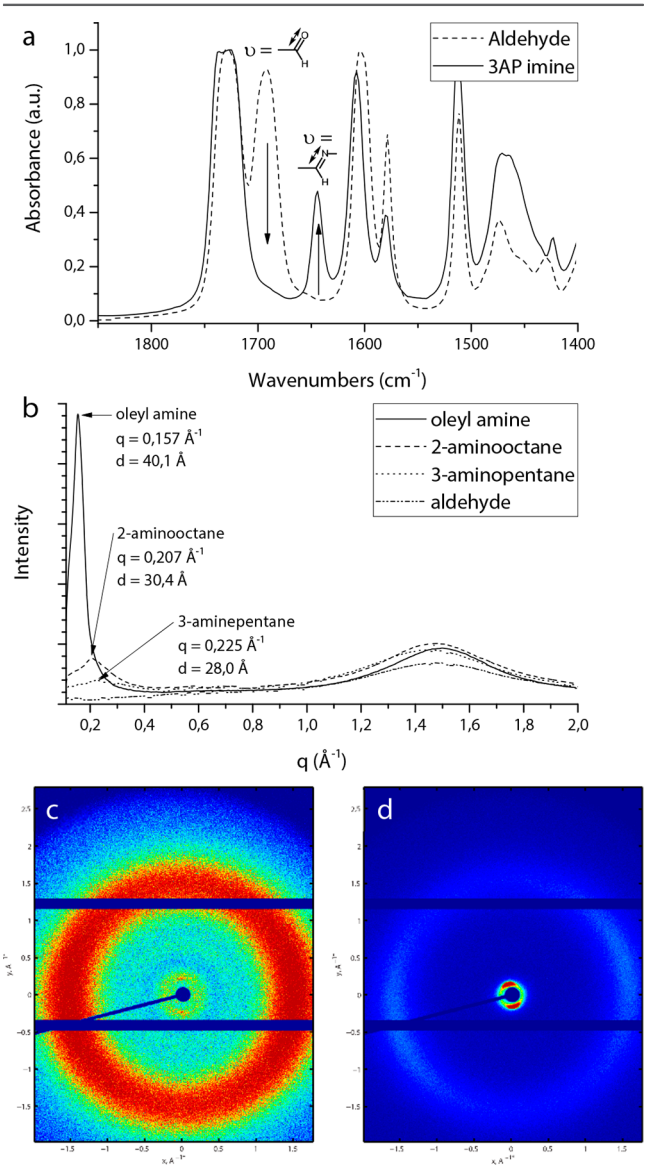

Figure 3. (a) FTIR spectrum of the aldehyde functional network (dashed) and the imine functional network (3-aminepentane, solid). (b) Azimuthal integration of the XRD patterns of the aldehyde (dotted) network and the networks treated with 3-aminopentane (short dash), 2-aminooctane (dashed), and oleylamine (solid). (c and d) 2D X-ray diffraction pattern of the 2-aminooctane and oleylamine treated network.

XRD measurement of the dry films demonstrates that a layer spacing of 28 and 30 Å was observed for the imine interiors of 3AP and 2AO, respectively, whereas for the much larger OA, with roughly twice the molecular weight of the initial diamine template, a layer spacing of 40 Å was found. We anticipate that the long flexible aliphatic chains interdigitate with the aliphatic side-chains of the mesogenic moieties because a relatively small layer spacing and a significantly higher scattering intensity is observed. Similar to the aliphatic amines, aromatic amines can be incorporated (SI Figure S6). When an aldehyde functional film is exposed to a solution containing equimolar amounts of aliphatic and aromatic amines, exclusively aliphatic amines are incorporated (SI Figure S7). We appoint this latter to the more nucleophilic nature of aliphatic amines.

Ultimately, the dynamic imine interior was fixed in by reducing the imines to secondary amines (Figure 4). This could either be accomplished by using sodium cyanoborohydride or, the milder and less toxic sodium triacetoxyborohydride. The secondary amine interior is stable and can be protonated to obtain a cationic charge inside the pore interior.

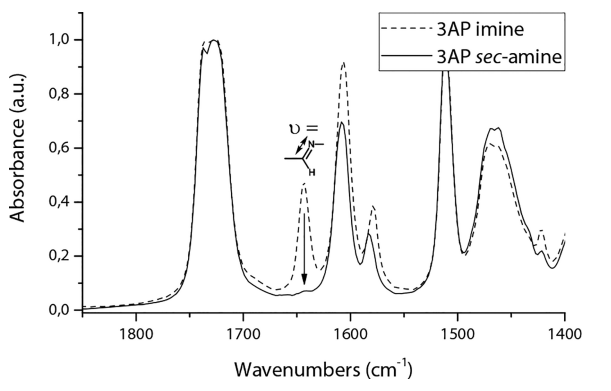

Figure 4. FTIR spectrum of the 3AP imine functional network (dashed) and the secondary amine functional network (solid).

As a proof of principle, the impact of the postmodification on the materials properties was demonstrated by the release of methyl orange from the 3AP and OA functionalized polymers. The use of dye is here convenient because of easy visualization. Prior to the desorption experiment, the films were first treated with 0.5 M HCl 1:1 water/THF to create a cationic pore interior by protonation of the sec-amine groups. Subsequently, the films containing 3AP and OA based *sec*-amines in their interior, are immersed in 3 mL solution containing 1 mg/mL MO in 1:1 (v/v) water/THF. The concentration in dye is such that there is a large excess when compared to the theoretical maximum capacity of the film that, based on only electrostatic interactions, is estimated at 616 mg/g and 373 mg/g for 3AP and OA, respectively. The 3AP sec-amine film was slightly darker orange compared to the OA film (Figure 5c).

To release the dye from the material, the films were placed in a cuvette containing 1 M HCl (Figure 5a). The film containing the 3AP *sec*-amine directly changed to a dark red color, followed by the release of the dye. The color change of the film indicates that HCl enters the network, protonating the MO dye before it was released. The film containing the oleyl amine did not change color. The long and interdigitated aliphatic tails of

DOI: 10.1021/acs.chemmater.7b01334
Chem. Mater. 2017, 29, 6601−6605

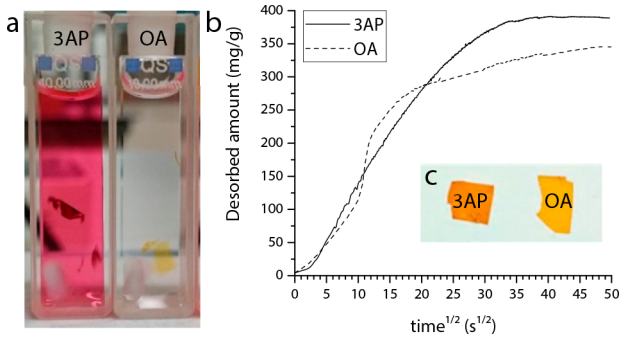

Figure 5. (a) Release of MO in 1 M HCl from 3AP film (left) and OA film (right). (b) Release of MO from a 3AP film (solid) and OA film (dashed) using 0.5 M HCl 1:1 (v/v) water/THF. (c) MO loaded films prior to desorption.

the oleylamine impede the transport of HCl into the material and accordingly prohibits the release of the dye. However, when 0.5 M HCl in 1:1 (v/v) THF/water was used as the solution, the dye could successfully be released from either of the *sec*-amine networks, although the kinetic profile both materials was found to be different (Figure 5b). The 3AP film shows a pseudo-Fickian release curve, indicating that the sorption is mainly diffusion controlled, where on the other hand, the OA material shows a two-stage release curve. This behavior is often observed in sorption in glassy polymers where the solvent interacts with the polymer. Such a curve is described as an anomalous transport mechanism where the release is driven by both diffusion and polymer relaxation.[26] The additional dis-interdigitation of the aliphatic OA tails inside the lamellae during the swelling in THF/water could be an explanation for this process. These results show that the chemical modification of the nanoporous interior in a polymer can be used to tune release of molecules.

CONCLUSIONS

We have developed a facile method to obtain lamellar nanoporous materials with an adjustable pore interior by using dynamic covalent imine chemistry. The reversibility of the bond makes the system appealing because the pore interior can be tuned on demand by in situ chemical modification. The obtained porous material is highly adaptive to the amine that is used to functionalize the pore interior. Indeed, amines with molecular weight up to double the molecular weight of the initial diamine template could be incorporated. Such results can potentially be used to control the size and chemical nature of the pores and the set of molecules and ions that can be separated by polymers. Finally, the dynamic character of the chemical bond in such polymers gives opportunities to create reusable and cleanable nanoporous materials.

ASSOCIATED CONTENT

Supporting Information

The Supporting Information is available free of charge on the ACS Publications website at DOI: 10.1021/acs.chemmater.7b01334.

Synthesis, experimental details, thermal characterizations, incorporation of aromatic compounds (PDF)

AUTHOR INFORMATION

Corresponding Author

*Albertus P. H. J. Schenning, e-mail: A.P.H.J.Schenning@tue.nl.

ORCID

Giuseppe Portale: 0000-0002-4903-3159

Albertus P. H. J. Schenning: 0000-0002-3485-1984

Present Address

[§]Surfix BV, Bronland 12 B-1, 6708 WH Wageningen, The Netherlands

Notes

The authors declare no competing financial interest.

ACKNOWLEDGMENTS

We thank Jody Lugger for the help with the XRD measurements. This research forms part of the research program of the Dutch Polymer Institute (DPI), project 776.

REFERENCES

(1) Jackson, E. A.; Hillmyer, M. A. Nanoporous Membranes Derived from Block Copolymers: From Drug Delivery to Water Filtration. *ACS Nano* **2010**, *4* (7), 3548−3553.

(2) van Kuringen, H. P. C.; Eikelboom, G. M.; Shishmanova, I. K.; Broer, D. J.; Schenning, A. P. H. J. Responsive Nanoporous Smectic Liquid Crystal Polymer Networks as Efficient and Selective Adsorbents. *Adv. Funct. Mater.* **2014**, *24* (32), 5045−5051.

(3) Kato, T.; Yoshio, M.; Ichikawa, T.; Soberats, B.; Ohno, H.; Funahashi, M. Transport of Ions and Electrons in Nanostructured Liquid Crystals. *Nat. Rev. Mater.* **2017**, *2*, 17001.

(4) Henmi, M.; Nakatsuji, K.; Ichikawa, T.; Tomioka, H.; Sakamoto, T.; Yoshio, M.; Kato, T. Self-Organized Liquid-Crystalline Nanostructured Membranes for Water Treatment: Selective Permeation of Ions. *Adv. Mater.* **2012**, *24* (17), 2238−2241.

(5) van Kuringen, H. P. C.; Leijten, Z. J. W. A.; Gelebart, A. H.; Mulder, D. J.; Portale, G.; Broer, D. J.; Schenning, A. P. H. J. Photoresponsive Nanoporous Smectic Liquid Crystalline Polymer Networks: Changing the Number of Binding Sites and Pore Dimensions in Polymer Adsorbents by Light. *Macromolecules* **2015**, *48* (12), 4073−4080.

(6) Feng, X.; Tousley, M. E.; Cowan, M. G.; Wiesenauer, B. R.; Nejati, S.; Choo, Y.; Noble, R. D.; Elimelech, M.; Gin, D. L.; Osuji, C. O. Scalable Fabrication of Polymer Membranes with Vertically Aligned 1 Nm Pores by Magnetic Field Directed Self-Assembly. *ACS Nano* **2014**, *8* (12), 11977−11986.

(7) Beck, J. S.; Vartuli, J. C.; Roth, W. J.; Leonowicz, M. E.; Kresge, C. T.; Schmitt, K. D.; Chu, C. T. W.; Olson, D. H.; Sheppard, E. W.; McCullen, S. B.; Higgins, J. B.; Schlenker, J. L. A New Family of Mesoporous Molecular Sieves Prepared with Liquid Crystal Templates. *J. Am. Chem. Soc.* **1992**, *114* (27), 10834−10843.

(8) Kresge, C. T.; Leonowicz, M. E.; Roth, W. J.; Vartuli, J. C.; Beck, J. S. Ordered Mesoporous Molecular Sieves Synthesized by a Liquid-Crystal Template Mechanism. *Nature* **1992**, *359* (6397), 710−712.

(9) Schenning, A. P. H. J.; Gonzalez-Lemus, Y. C.; Shishmanova, I. K.; Broer, D. J. Nanoporous Membranes Based on Liquid Crystalline Polymers. *Liq. Cryst.* **2011**, *38* (11−12), 1627−1639.

(10) Ichikawa, T.; Yoshio, M.; Hamasaki, A.; Mukai, T.; Ohno, H.; Kato, T. Self-Organization of Room-Temperature Ionic Liquids Exhibiting Liquid-Crystalline Bicontinuous Cubic Phases: Formation of Nano-Ion Channel Networks. *J. Am. Chem. Soc.* **2007**, *129* (35), 10662−10663.

(11) Zhou, M.; Nemade, P. R.; Lu, X.; Zeng, X.; Hatakeyama, E. S.; Noble, R. D.; Gin, D. L. New Type of Membrane Material for Water Desalination Based on a Cross-Linked Bicontinuous Cubic Lyotropic Liquid Crystal Assembly. *J. Am. Chem. Soc.* **2007**, *129* (31), 9574−9575.

DOI: 10.1021/acs.chemmater.7b01334
Chem. Mater. 2017, 29, 6601−6605

(12) Gin, D. L.; Noble, R. D. Designing the Next Generation of Chemical Separation Membranes. *Science* **2011**, *332* (6030), 674−676.
(13) Gracia, I.; Romero, P.; Serrano, J. L.; Barberá, J.; Omenat, A. Templated Nanoporous Membranes Based on Hierarchically Self-Assembled Materials. *J. Mater. Chem. C* **2017**, *5* (8), 2033−2042.
(14) Li, C.; Cho, J.; Yamada, K.; Hashizume, D.; Araoka, F.; Takezoe, H.; Aida, T.; Ishida, Y. Macroscopic Ordering of Helical Pores for Arraying Guest Molecules Noncentrosymmetrically. *Nat. Commun.* **2015**, *6*, 8418.
(15) Kishikawa, K.; Hirai, A.; Kohmoto, S. Fixation of Multilayered Structures of Liquid-Crystalline 2:1 Complexes of Benzoic Acid Derivatives and Dipyridyl Compounds and the Effect of Nanopillars on Removal of the Dipyridyl Molecules from the Polymers. *Chem. Mater.* **2008**, *20* (5), 1931−1935.
(16) Lee, H.-K.; Lee, H.; Ko, Y. H.; Chang, Y. J.; Oh, N.-K.; Zin, W.-C.; Kim, K. Synthesis of a Nanoporous Polymer with Hexagonal Channels from Supramolecular Discotic Liquid Crystals. *Angew. Chem., Int. Ed.* **2001**, *40* (14), 2669−2671.
(17) Gonzalez, C. L.; Bastiaansen, C. W. M.; Lub, J.; Loos, J.; Lu, K.; Wondergem, H. J.; Broer, D. J. Nanoporous Membranes of Hydrogen-Bridged Smectic Networks with Nanometer Transverse Pore Dimensions. *Adv. Mater.* **2008**, *20* (7), 1246−1252.
(18) Wiesenauer, B. R.; Gin, D. L. Nanoporous Polymer Materials Based on Self-Organized, Bicontinuous Cubic Lyotropic Liquid Crystal Assemblies and Their Applications. *Polym. J.* **2012**, *44* (6), 461−468.
(19) Giuseppone, N.; Lehn, J.-M. Protonic and Temperature Modulation of Constituent Expression by Component Selection in a Dynamic Combinatorial Library of Imines. *Chem. - Eur. J.* **2006**, *12* (6), 1715−1722.
(20) Baxter, P. N. W.; Khoury, R. G.; Lehn, J.-M.; Baum, G.; Fenske, D. Adaptive Self-Assembly: Environment-Induced Formation and Reversible Switching of Polynuclear Metallocyclophanes. *Chem. - Eur. J.* **2000**, *6* (22), 4140−4148.
(21) Ciesielski, A.; El Garah, M.; Haar, S.; Kovaříček, P.; Lehn, J.-M.; Samorì, P. Dynamic Covalent Chemistry of Bisimines at the Solid/Liquid Interface Monitored by Scanning Tunnelling Microscopy. *Nat. Chem.* **2014**, *6* (11), 1017−1023.
(22) Roy, N.; Bruchmann, B.; Lehn, J.-M. Dynamer: Dynamic Polymers as Self-Healing Materials. *Chem. Soc. Rev.* **2015**, *44* (11), 3786−3807.
(23) Bhattacharjee, S.; Lugger, J. A. M.; Sijbesma, R. P. Tailoring Pore Size and Chemical Interior of near 1 Nm Sized Pores in a Nanoporous Polymer Based on a Discotic Liquid Crystal. *Macromolecules* **2017**, *50* (7), 2777−2783.
(24) Piñol, R.; Lub, J.; García, M. P.; Peeters, E.; Serrano, J. L.; Broer, D.; Sierra, T. Synthesis, Properties, and Polymerization of New Liquid Crystalline Monomers for Highly Ordered Guest−Host Systems. *Chem. Mater.* **2008**, *20* (19), 6076−6086.
(25) Kußerow, J.; Boberg, F. Symmetrische Flüssigkristalline Bibenzyl-4,4′-Diylbisbenzoate, Synthese Und Charakterisierung [1,2]. *J. Prakt. Chem./Chem.-Ztg.* **1994**, *336* (7), 613−616.
(26) Bond, D. A.; Smith, P. A. Modeling the Transport of Low-Molecular-Weight Penetrants Within Polymer Matrix Composites. *Appl. Mech. Rev.* **2006**, *59* (5), 249−268.

DOI: 10.1021/acs.chemmater.7b01334
Chem. Mater. 2017, 29, 6601−6605